

## Original Article

## Caffeine enhances chemosensitivity to irinotecan in the treatment of colorectal cancer

Seobin Yoon<sup>a</sup>, Bum-Kyu Lee<sup>b</sup>, Keun Pil Kim<sup>a,\*</sup><sup>a</sup> Department of Life Sciences, Chung-Ang University, Seoul 06974, South Korea<sup>b</sup> Department of Biomedical Sciences, Cancer Research Center, University of Albany-State University of New York, Rensselaer, NY, USA

## ARTICLE INFO

## Keywords:

Colorectal cancer  
Irinotecan  
Caffeine  
Rad51  
DNA repair

## ABSTRACT

**Background:** Colorectal cancer (CRC) is one of the most common types of cancer. This disease arises from gene mutations and epigenetic alterations that transform colonic epithelial cells into colon adenocarcinoma cells, which display a unique gene expression pattern compared to normal cells. Specifically, CRC cells exhibit significantly higher expression levels of genes involved in DNA repair or replication, which is attributed to the accumulation of DNA breakage resulting from rapid cell cycle progression.

**Purpose:** This study aimed to investigate the *in vivo* effects of caffeine on CRC cells and evaluate its impact on the sensitivity of these cells to irinotecan, a topoisomerase I inhibitor widely used for CRC treatment.

**Methods:** Two CRC cell lines, HCT116 and HT29, were treated with irinotecan and caffeine. Western blot analysis assessed protein expression levels in caffeine/irinotecan-treated CRC cells. Immunofluorescence staining determined protein localization, measured DNA breaks, and explored the effects of DNA damage reagents during cell cycle progression and flow cytometry analysis was used to measure cell viability. Fiber assays investigated DNA synthesis in DNA-damaged cells during S-phase, while the comet assay assessed DNA fragmentation caused by DNA breaks.

**Results:** Our findings demonstrated that the combination of irinotecan and caffeine exhibits a synergistic effect in suppressing CRC cell proliferation and inducing cell death. Compared to treatment with only irinotecan or caffeine, the combined irinotecan and caffeine treatment was more effective in inducing DNA lesions by displacing RAD51 from DNA break sites and inhibiting DNA repair progression, leading to cell cycle arrest. This combination also resulted in more severe effects, including DNA fragmentation and mitotic catastrophe.

**Conclusion:** Caffeine could enhance the effectiveness of an existing drug for CRC treatment despite having little impact on the cell survival rate of CRC cells. Our findings suggest that the beneficial adjuvant effects of caffeine may not only be applicable to CRC but also to various other types of cancers at different stages of development.

## Introduction

DNA repair and recombination are essential processes that suppress cancer formation resulting from genetic mutations (Friedberg, 2001; Hanahan and Weinberg, 2011). Moreover, the inactivation of DNA repair mechanisms at distinct stages of DNA damage inhibits the DNA replication and proliferation capacity of cancer cells (Hanahan and Weinberg, 2011; Aguilera and Gómez-González, 2008; Helleday et al., 2008). However, DNA repair factors are known to be overexpressed in

colorectal cancer (CRC) cells make them highly resilient to DNA damage (Choi and Kim, 2019; Vispé et al., 1998). Specifically, CRC cells employ a modified homologous recombination (HR) mechanism to rescue cell cycle arrest and apoptosis in response to various stresses (Zhou et al., 2020). Previous studies have been conducted to control the genetic information of CRC cells. However, efficiently inducing apoptosis in CRC cells during the treatment stage remains a significant challenge (Kerr, 2003; Cremolini et al., 2015). Changes in the gene repair protein network found in CRC cell lines are a key factor that greatly affects cell

**Abbreviations:** CRC, colorectal cancer; DSB, double-strand break; HR, homologous recombination; Topo I, topoisomerase I; Top1cc, topoisomerase 1 cleavage complex; ICLs, interstrand crosslinks; ATM, ataxia-telangiectasia mutated; ATR, ataxia telangiectasia and Rad3-related; DNA-PK, DNA-dependent protein kinase; D-loop, displacement-loop.

\* Corresponding author.

E-mail address: [kpkim@cau.ac.kr](mailto:kpkim@cau.ac.kr) (K.P. Kim).

<https://doi.org/10.1016/j.phymed.2023.155120>

Received 26 March 2023; Received in revised form 5 September 2023; Accepted 27 September 2023

Available online 28 September 2023

0944-7113/© 2023 The Author(s). Published by Elsevier GmbH. This is an open access article under the CC BY-NC license (<http://creativecommons.org/licenses/by-nc/4.0/>).

mutation and cancer cell activity; therefore, further research is urgently needed to clarify this process, which would aid in the creation of novel diagnosis and treatment strategies for CRC (Helleday et al., 2008). In addition to the development of various treatments to increase the effectiveness of CRC treatments, further efforts are needed to maximize the effectiveness of existing treatments (Xie et al., 2020). To this end, we proposed a cultured cell-based approach that can be applied to assess the effects of genetic damage not only on CRC cells but also on various other cancer cell types.

CRC cells exhibit elevated expression of genes involved in DNA repair or replication, such as RAD51 and topoisomerase, in comparison to normal cells (Choi and Kim, 2019; Rømer et al., 2012). Chemotherapeutic agents often disrupt the factors related to DNA repair or replication, as such inhibition induces cellular stress, ultimately leading to genomic instability and heightened sensitivity of cancer cells to drug interventions (Li et al., 2021). Irinotecan is a commonly used cytotoxic chemotherapy drug for metastatic CRC (Pommier, 2006). This drug is a semisynthetic analog derived from camptothecin, a phytochemical derived from the Chinese tree *Camptotheca acuminata*, which inhibits topoisomerase I activity in diverse stages of DNA metabolism (Pommier et al., 2006, 2010). Topoisomerase I (Topo I) unwinds DNA strands during DNA replication and transcription by cleaving single-strand DNA to inhibit the formation of supercoiled DNA (Pommier, 2006; Pommier et al., 2010; Champoux, 1981). Topoisomerase I (Topo I) possesses a catalytic tyrosine residue (Y723 in human Topo I) containing a phenolic OH group. This group forms a DNA-Topo I covalent complex by attacking the phosphate ester, a process known as transesterification, which is reversible (Pommier, 2006; Champoux, 1981). Once a covalent bond is established, a DNA strand with a free 5'-OH group is generated, leading to relaxation of DNA supercoiling. Following the removal of supercoiled DNA, Topo I facilitates the rejoining of DNA strands through nucleophilic attack on the tyrosyl-DNA bond by the free DNA end (Pommier, 2006).

Irinotecan inhibits the Topo I enzyme, causing DNA damage and ultimately inducing cell death in rapidly dividing cancer cells (Pommier, 2006). The resulting trinary complex stabilizes into a Topo I cleavage complex, preventing the topoisomerase from mediating DNA religation and releasing Topo I from the broken DNA end (Pommier, 2006; Thomas and Pommier, 2019). Accumulation of this complex leads to the generation of double-strand breaks (DSBs) during replication (Strumberg et al., 2000). Consequently, irinotecan instigates DNA breaks followed by replication arrest and eventual cell death (Xu and Villalona-Calero, 2002; Stenvang et al., 2013). Various factors are involved during DNA repair or replication, including topoisomerase, RAD51, or RPA (Pommier, 2006; Strumberg et al., 2000; Choi et al., 2017a; Choi et al., 2018, 2020). Particularly, RAD51 is a critical protein involved in various processes such as homologous recombination (HR), DNA replication, stem cell differentiation, and enhancing CRISPR-Cas9 efficiency (Choi et al., 2017b; Choi et al., 2018; Choi et al., 2020; Park et al., 2023). During HR-mediated DNA repair, which is a type of DNA repair pathway to repair double-strand DNA breaks, RAD51 facilitates the exchange of genetic material between the broken DNA molecule and an undamaged DNA molecule, resulting in break repair (Li and Heyer, 2008; Krejci et al., 2012). RAD51 achieves this by binding to single-stranded DNA at the site of the DSB and promoting the search for a homologous DNA sequence (Li and Heyer, 2008). This mechanism engages in faithful genome duplication resulting from DNA replication and repairing DNA lesions such as DSBs, DNA gaps, and DNA interstrand crosslinks (ICLs) (Li and Heyer, 2008; Krejci et al., 2012). Previous studies have examined the functional characteristics of factors related to RAD51, a key DNA repair factor that plays a crucial role in maintaining the genome stability of CRC cells. Particularly, these factors were identified as target markers by analyzing changes in chromosome structure and the dynamic characteristics of proteins (Manic et al., 2021; Tennstedt et al., 2013). When the expression of RAD51 is suppressed, CRC cells exhibit alterations in DNA replication and repair, resulting in

induction of apoptosis and inhibition of cell proliferation (Feu et al., 2022). As mentioned above, RAD51 plays a crucial role in the HR-mediated DNA repair pathway, which is important for repairing DNA damage and maintaining genome integrity (Li and Heyer, 2008; Krejci et al., 2012; Feu et al., 2022). However, RAD51 is known to be overexpressed in cancer cells such as CRC cells, which can increase DNA repair capacity and contribute to cancer development and progression (Tennstedt et al., 2013; Feu et al., 2022). Therefore, targeting RAD51 could be an effective strategy for inhibiting the proliferation of CRC cells.

Caffeine, a purine alkaloid, is widely present in a wide variety of plant-derived products such as coffee beans and tea leaves (Tsabar et al., 2015; Zelensky et al., 2013; Bode and Dong, 2007). Furthermore, caffeine has been reported to inhibit the HR factor RAD51 by displacing the recombinase from the ssDNA filaments, ATM (ataxia-telangiectasia mutated), or ATR (ataxia telangiectasia and Rad3-related), thus affecting cell cycle progression and HR mechanisms and inducing apoptosis (Tsabar et al., 2015; Zelensky et al., 2013; Choi et al., 2017a; Bode and Dong, 2007). The adjuvant effect of caffeine in cancer treatment is a topic of ongoing research. Some studies have suggested that caffeine may enhance the effectiveness of certain cancer chemotherapies by increasing the uptake and accumulation of chemotherapeutic drugs in tumor cells (Bode and Dong, 2007; Wang et al., 2015). However, these results are still preliminary, and adjuvant approaches are needed to fully understand the potential adjuvant effects of caffeine in cancer treatment. Additionally, it is important to note that caffeine should only be used as a complementary treatment for cancer under the supervision of a qualified healthcare provider.

In this study, we have demonstrated the synergistic effects of combining irinotecan and caffeine to induce DNA breaks and promote cell death in CRC cells, specifically HCT116 and HT29. The combination of irinotecan and caffeine heightened the expression of  $\gamma$ H2AX, a marker for DSBs, by disrupting RAD51 function in both the HCT116 and HT29 cell lines, despite RAD51 protein levels remaining consistent in the presence or absence of caffeine. Co-treatment with irinotecan and caffeine led to a decelerated progression of the cell cycle and suppressed DNA replication. Additionally, we evaluated DNA breaks and the viability of CRC cells under each experimental condition. While treatment with either caffeine or irinotecan alone induced some level of DNA breaks and apoptosis, the combined application of these drugs yielded substantially greater increases in both these outcomes. In summary, the results illuminate caffeine's potential to augment the effectiveness of irinotecan, a chemotherapy medication commonly employed for treating CRC.

## Materials and methods

### Colorectal cell culture and induction of DNA damage

The HCT116 and HT29 cell lines were cultured and maintained as described previously (Choi and Kim, 2019). Both cell lines were cultured in DMEM (Dulbecco's modified Eagle medium; Cat.11995-073, Gibco) supplemented with heat-inactivated 10% FBS (fetal bovine serum; Cat.16000-044, Gibco) and 1 % penicillin/streptomycin (PS; Cat.15140-122, Gibco). The cells were then incubated in a humidified environment with 5% CO<sub>2</sub> at 37°C. To generate DNA breaks, the culture medium was treated with 5 mM caffeine (Cat.C0750, Sigma, purity (HPLC)  $\geq$  99.0%) for 4 h (Bode and Dong, 2007; Han et al., 2011; Qi et al., 2022), after which 30  $\mu$ g/ml irinotecan (Cat.I1406, Sigma, purity (HPLC)  $\geq$  97.0%) was added to the culture medium and the cells were incubated for an additional 12 h (Zhang et al., 2019).

### Immunoblot analysis

The samples for immunoblot analysis were prepared as described in a previous study (Yoon et al., 2014). The samples were washed twice with

PBS and lysed using cell lysis buffer supplemented with a proteinase inhibitor cocktail (PIC) and 1 mM phenylmethylsulfonyl fluoride (PMSF). The primary antibodies used in this study were as follows: RAD51 (Cat.PC130, Merck Millipore, diluted at 1:3000), and  $\alpha$ -tubulin (Cat.ab4074, Abcam, diluted at 1:10,000). The HRP (horseradish peroxidase)-conjugated secondary antibodies were obtained from Jackson ImmunoResearch Laboratories (Cat.111–035–003). The expression level of each protein was quantified using the Bio-Rad Image Lab software.

#### Immunofluorescence analysis

Cells were attached on poly-L-lysine coated coverslips and fixed with 4% paraformaldehyde. The fixed cells were permeabilized using 0.2% Triton X-100. The samples were then blocked with 0.1% bovine serum albumin (BSA) in phosphate-buffered saline supplemented with 0.02% Tween 20 (PBS-T), after which they were treated and incubated for 1 hour with RAD51 (1:200) and  $\gamma$ H2AX (1:500) primary antibodies. The secondary antibodies [anti-rabbit tetramethylrhodamine (TRITC)-conjugated antibody (Cat. 111–025–144, Jackson, 1:500)] were then added after washing the antibody-bound samples three times with PBS-T. Next, the stained samples were covered with an antifade mounting solution with DAPI (Cat. P36935, Thermo Scientific). Finally, the samples were examined and photographed using a Nikon Eclipse Ti-E inverted microscope equipped with a Nikon DS-Qi2 camera with a 100 $\times$  lens and 100 $\times$  oil objective, and the images were analyzed using the NIS software from Nikon.

#### Fluorescence-activated cell sorting (FACS) analysis

Cell viability assays were conducted as described in a previous study (Yoon et al., 2023). The cells were harvested and washed with PBS. Next, 84 nM thiazole orange (TO, Cat.349483, BD) and 4.3  $\mu$ M propidium iodide (PI, Cat.349483, BD) were added to the samples. Afterward, the samples were incubated at room temperature and then analyzed using a BD Accuri C6 cytometer (BD Biosciences). The data were analyzed using the Accuri C6 software (BD Bioscience). For cell cycle analysis, the cells were fixed with 70% ethanol overnight. Finally, the fixed cells were harvested and stained with PI and the cell cycle patterns were profiled using a flow cytometer (BD FACS Calibur).

#### Fiber assay

The samples for the fiber assay were prepared as described in a previous study (Choi et al., 2022). Cells under each condition were treated with 50  $\mu$ M 5-Iodo-2'-deoxyuridine (IdU, Cat. GP1769, Glenham) for 15 min and washed twice with PBS, followed by treatment with 100  $\mu$ M 5-chloro-2'-deoxyuridine (CldU, Cat. C6891, Sigma) for 15 min. After treatment with thymidine analogs, the cells were harvested and then resuspended in chilled PBS. The concentration of the samples was adjusted to 400 cells/ $\mu$ l, after which they were mounted on slide glasses. For DNA lysis, lysis buffer (200 mM Tris-HCl pH 7.4, 0.5% SDS, and 50 mM EDTA) was added to the cells. The slide glasses were tilted to spread the DNA, after which the samples were allowed to dry for 30 min. After drying, the samples were fixed using methanol/acetic acid (3:1 v/v) for 10 min and allowed to dry overnight at room temperature. The dried slides were immersed in 2.5 N HCl for 1 h, after which the immersed samples were blocked with 1% BSA in PBS, followed by primary antibody staining with IdU-specific (Cat. B44, BD, 1:25) and CldU-specific antibodies (Cat. ab6326, Abcam, 1:500). After washing with PBS-T (0.1% Tween 20 in PBS), the samples were incubated with secondary antibodies: TRITC-labeled goat anti-mouse IgG antibody (Cat. 115–025–003, Jackson ImmunoResearch; 1:300) to detect IdU and FITC-conjugated goat anti-rat IgG antibody (Cat. 112–095–003, Jackson ImmunoResearch; 1:400) to detect CldU. The stained cells were washed with PBS-T and mounted with an antifade mounting solution with DAPI.

Fiber assay images were captured using fluorescence microscopy (Nikon Eclipse, Ti-E) and the lengths of the fibers were measured with the Nikon NIS software.

#### Comet assay

The harvested cells were suspended and mixed with 1% agarose gel (42°C). The mixture of cells and gel was then set on glass slides and allowed to solidify, after which the solidified gels were immersed in lysis buffer [2% sarcosyl and 0.5 M Na<sub>2</sub>EDTA (pH 8.0) including 0.5 mg/ml Proteinase K, pH 8.0] for 20 h. After lysis, the slides were rinsed with buffer [90 mM Tris, 90 mM boric acid, and 2 mM Na<sub>2</sub>EDTA, pH 8.5] via submersion for 30 min. Electrophoresis was conducted for 25 min at 20 V. Afterward, the gels were stained with 2.5  $\mu$ g/ml PI in PBS for 20 min. Images were captured via fluorescence microscopy, and the tail of the comet was measured with the CASP software ver. 1.2.3 beta2 (CaspLab).

#### WST-8 assay

The WST-8 (Water-soluble tetrazolium-8) assay was used to determine the effects of irinotecan or 5-FU in combination with caffeine. The assay was performed according to the manufacturer's protocol. Cells were inoculated in a 96-well plate (100  $\mu$ l/well) and pre-incubated in a 37 °C humidified incubator with 5% CO<sub>2</sub>. Both cell lines were then subjected to multiple treatments, including 5-FU (Cat. F6627, Sigma-Aldrich) at concentrations of 0, 1, 10, 25, 50, and 100  $\mu$ M for 48 h (de Castro e Gloria et al., 2021) and irinotecan at concentrations of 0, 5, 10, 20, 30, 50, and 100  $\mu$ g/ml for 12 h (Zhang et al., 2019). The IC<sub>50</sub> value was then calculated from the acquired data and graphs were generated using GraphPad Prism software 9.

#### RNAi

Small interfering RNAs (siRNAs) against RAD51 and a negative control (SN-1003) were pre-designed and prepared by Bioneer. 150 nM siRNAs mixed with opti-MEM medium (Gibco) were then transfected with Lipofectamine RNAiMAX (Thermo Fisher). Finally, the siRNA-treated cells were incubated for 48 h in an incubator at 37°C with 5% CO<sub>2</sub>. The siRNA against RAD51 had the following sequence: 5'-GAAUUGAGACUGGAUCUAU-3'.

#### Statistical analysis

All statistical analyses were conducted as described previously (Koh et al., 2022). All data were analyzed with the GraphPad Prism 5 software and reported as averages  $\pm$  SD (standard deviation). Statistically significant differences between the control and experimental groups were determined via paired two-tailed *t*-tests. *P*-values were calculated using the GraphPad Prism 5 software (\**p* < 0.05, \*\**p* < 0.01, and \*\*\**p* < 0.001).

## Results

### Caffeine acts as an inhibitor of RAD51 without altering RAD51 expression

RAD51 expression level is much higher in CRC cells than in normal cells, making them more resistant to chemotherapeutic drugs and radiotherapy (Vispé et al., 1998; Zhou et al., 2020). Previous studies have indicated that caffeine can act as an inhibitor of RAD51 function by displacing it from DNA gaps during DNA breaks caused by various processes such as DNA replication, chemotherapy, or radiation (Fig. 1) (Tsabar et al., 2015; Zelensky et al., 2013). We first analyzed the expression level of RAD51 when CRC cells (HCT116 and HT29) were treated with 5 mM caffeine for 4 h (Bode and Dong, 2007; Han et al., 2011; Qi et al., 2022). Our findings revealed that the protein level of RAD51 remained similar regardless of caffeine treatment, suggesting

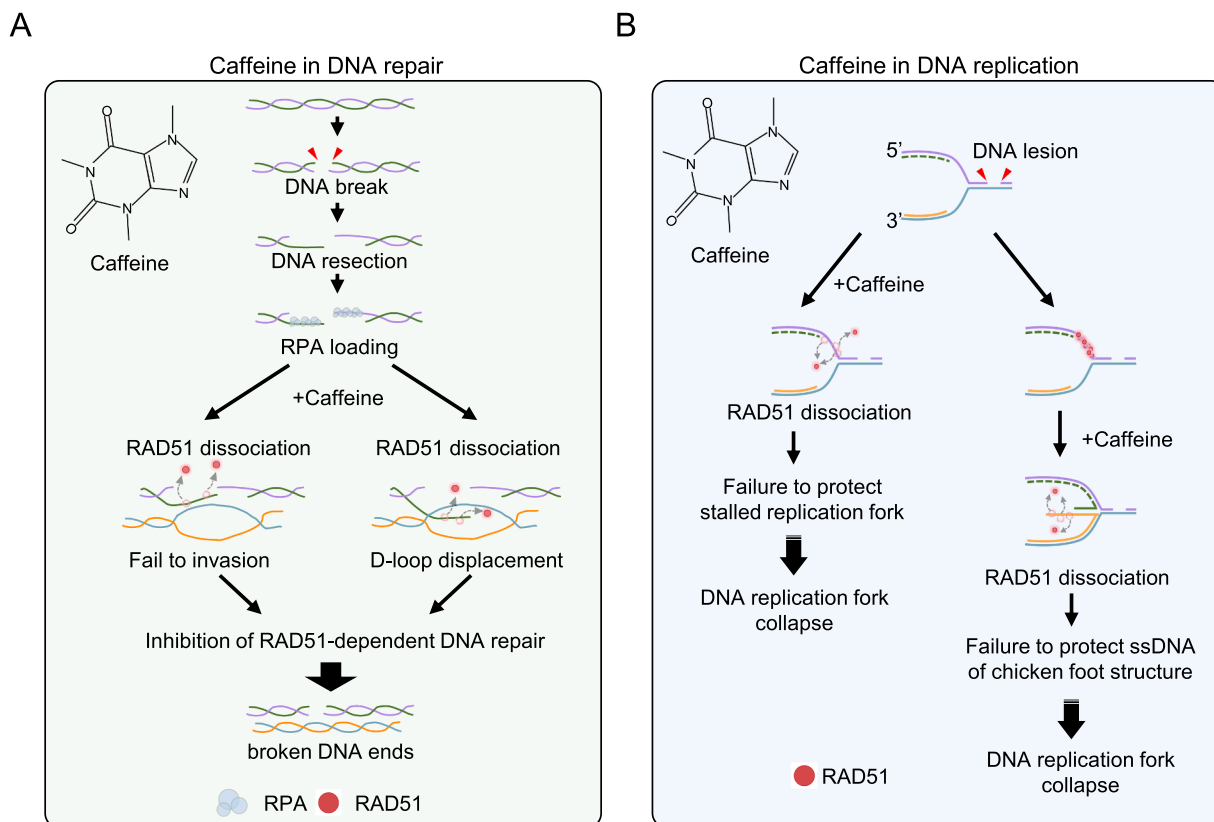


**Fig. 1.** Effects of caffeine on DNA repair progression and DNA replication. (A, B) Schematic representation of the effects of caffeine. After the generation of DNA lesions, the broken DNA is resected by nucleases, thus exposing single-stranded DNAs (ssDNAs). Replication protein A (RPA) localizes on the exposed DNA to inhibit the formation of secondary structures of ssDNAs. Nucleoprotein filaments are formed through the exchange from RPA to RAD51 via several mediators that search for homology. The filaments then invade a homologous template and are elongated by DNA synthesis. The extended ssDNA is filled by ligation, thus completing the DNA repair mechanism. When cells are treated with caffeine, it dissociates the recombinase from the nucleoprotein filament or interrupts RAD51 binding to ssDNA generated by DNA breaks. Inhibition of RAD51 function results in an incomplete repair mechanism, leading to the persistence of DNA breaks (A). Additionally, during DNA replication, RAD51 is involved in the restarting process in response to stress. RAD51 protects DNA by binding onto the stalled replication fork and enhances the regression of the replication fork, thus forming a chicken foot-shaped structure. Disrupting RAD51 function by displacing it from the nucleoprotein filaments causes the collapse of the replication fork (B).

that inducing DNA breaks does not affect RAD51 protein expression, as it is already abundantly expressed (Fig. 2A). However, RAD51 focus formation was decreased in the two types of colorectal cancer cells, whereas focus formation of the DNA damage marker  $\gamma$ H2AX was much higher in the caffeine-treated HCT116 and HT29 cells than in both control cells (Fig. 2B). These findings indicate that caffeine induces the accumulation of DNA breaks by inhibiting DNA repair, leading to the dissociation of RAD51 from the breaks despite its high expression levels.

Irinotecan, a commonly used solid tumor drug, acts as a first-line treatment by inhibiting Topo I (Fig. 2C and D) (Pommier, 2006; Thomas and Pommier, 2019). Topo I plays a critical role in DNA replication, transcription, and repair by cleaving single-strand DNA to unwind DNA and maintain genomic stability. Additionally, due to the high expression of Topo I in CRC cells, CRC is hypersensitive to irinotecan, which attacks Top1cc, inhibits the religation of DNA strands, and leads to DNA breaks (Fig. 2D) (Rømer et al., 2012). The CRC cells were treated with irinotecan with or without caffeine to analyze whether these two reagents act synergistically on cancer cells. First, the expression of RAD51 was quantified in HCT116 cells and HT29 cells treated with irinotecan and irinotecan + caffeine. In the irinotecan-treated HCT116 cells, the RAD51 expression level was similar to that of the control cells. RAD51 expression remained similar in HCT116 and HT29 CRC cell lines, irrespective of treatment with irinotecan, caffeine, or irinotecan + caffeine, indicating that RAD51 expression is not influenced by these DNA damage agents (Fig. 2E and F).

#### Disruption of DNA repair progression by displacing RAD51 from breaks

RAD51 expression remained unchanged regardless of treatment with DNA damage agents (Fig. 2E and F). However, unlike RAD51 protein expression, RAD51 focus formation was not similar in DNA-damaged cancer cells. The number of RAD51 foci decreased when both the HCT116 and HT29 cell lines were treated with caffeine. In the HCT116 cells, the number of foci of the HR factor was  $2.48 \pm 2.50$  in the control group and  $0.79 \pm 1.24$  in the caffeine-treated group. Similarly, in the HT29 cell line, the number of RAD51 foci was  $2.47 \pm 2.25$  in the control group and  $1.04 \pm 1.29$  in the caffeine-treated group (Fig. 3A–D). However, caffeine induced DNA damage and the expression of  $\gamma$ H2AX, a DNA break marker, in both CRC cell lines. In the control cells of each cell line, the foci number of the DNA break marker was  $8.33 \pm 5.45$  in HCT116 cells and  $10.14 \pm 7.64$  in HT29 cells (Fig. 3A, B, E and F). In caffeine-damaged HCT116 cells, the  $\gamma$ H2AX foci number was  $33.15 \pm 11.09$ , whereas in caffeine-treated HT29 cells, the foci number was  $37.46 \pm 14.94$ , indicating that caffeine induces the generation of DNA breaks by inhibiting RAD51 localization on DNA gaps (Fig. 3A, B, E, F). In both cell lines treated with irinotecan, RAD51 focus formation was increased 32.8-fold compared to the control cells in the HCT116 cell line and 41.2-fold compared to the control HT29 cells (Fig. 3A–D). Additionally, the formation of  $\gamma$ H2AX foci was dramatically increased in the irinotecan-treated cells. In the control cells,  $\gamma$ H2AX expression exhibited a dot-like pattern, whereas  $\gamma$ H2AX was widely distributed throughout the chromatin under the DNA damage condition (irinotecan-treated

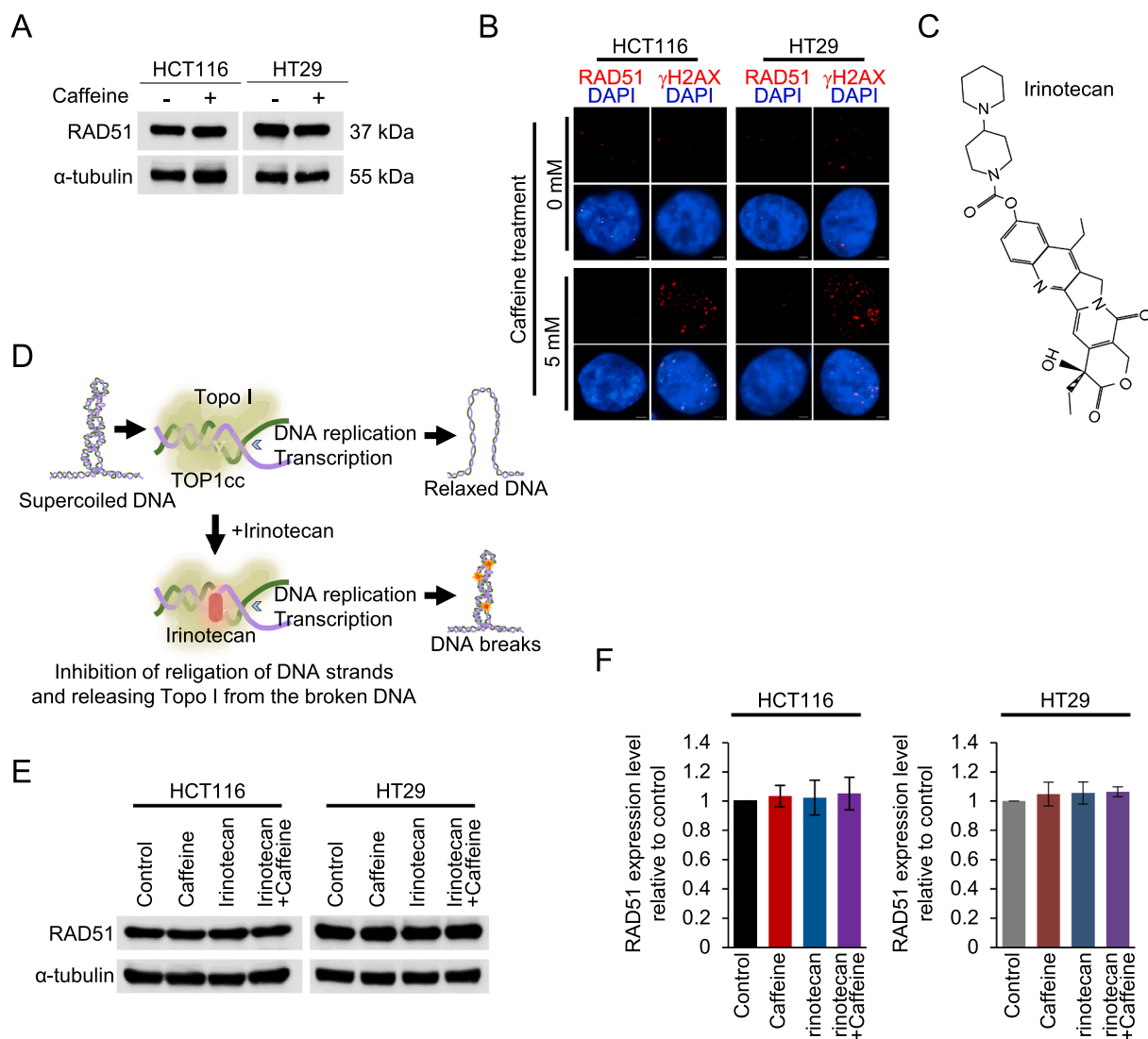


**Fig. 2.** RAD51 protein expression remained unchanged regardless of caffeine or irinotecan treatment. (A) RAD51 expression level with/without caffeine. Both cell lines, HCT116 and HT29, were treated with 0 mM caffeine in the same volume of PBS as in the 5 mM caffeine treatment for 4 h. (B) Focus formation of RAD51 and  $\gamma$ H2AX in caffeine-treated CRC cells. The cells were treated with either caffeine 0 mM (the same volume of PBS as in the 5 mM caffeine) or caffeine 5 mM (5 mM caffeine dissolved in PBS) for 4 h. Scale bars = 2.5  $\mu$ m. (C) Chemical structure of irinotecan. (D) Relaxation of the supercoiled form of DNA by Topo I and interruption of Topo I by irinotecan. Topo I unwinds supercoiled DNA by inducing DNA breaks caused by transesterification between the DNA strand and the tyrosine residue of Topo I. The complex generated by the tyrosine-DNA phosphodiester bond is called Top1cc. Topo I activity is inhibited by irinotecan via trapping the Top1cc, thus leading to DNA lesions. (E) RAD51 expression level. In each condition [control (DMSO and PBS), caffeine (5 mM caffeine and DMSO), irinotecan (30  $\mu$ g/ml irinotecan and PBS), and irinotecan + caffeine (30  $\mu$ g/ml irinotecan and 5 mM caffeine)], RAD51 expression was confirmed via western blot. (F) Quantification of the expression level of RAD51 factor. Three independent experiments were performed and the RAD51 expression levels in each condition in (E) were quantified using the BioRad software.

cells) (Fig. 3A, B, E and F). The  $\gamma$ H2AX intensity was  $45.08 \pm 3.47$  in the irinotecan-treated HCT116 cells and  $45.50 \pm 14.97$  in the irinotecan-treated HT29 cells (Fig. 3E and F). Our findings demonstrated that irinotecan was critical for the disruption of the genome stability of CRC cells by hindering Topo I function, thereby inducing DNA damage. Moreover, when the cells were treated with both caffeine and irinotecan,  $\gamma$ H2AX intensity was increased by 75.91% in HCT116 and 34.17% in HT29 compared to the CRC cells treated with irinotecan only. In contrast, RAD51 focus formation was significantly reduced to 75.95% in HCT116 and 60.51% in HT29 cells treated with irinotecan + caffeine compared to the CRC cells treated with irinotecan only (Fig. 3C–F). Collectively, these results suggest that caffeine induces DNA breaks and disrupts proper DNA repair progression by displacing RAD51 from the DNA damage sites generated by DNA damage agents.

#### Inhibition of Topo I and RAD51 function changes cell cycle progression

Camptothecin and camptothecin derivatives including irinotecan are generally known to induce cell cycle arrest at the G2/M phase due to a structural change near the active site upon binding (Pommier, 2006). Caffeine affects cell cycle progression by initiating the checkpoint response, thereby blocking ATM and ATR, and preventing RAD51 from binding to exposed single-strand DNA during DNA replication (Tsabar et al., 2015; Bode and Dong, 2007). A previous study further reported that caffeine arrests the cell cycle progression at the G1/S phase and abrogates or reverses the G1/S and G2/M checkpoint delay (Bode and Dong, 2007). Moreover, the co-administration of caffeine with other DNA-damaging agents significantly intensifies DNA damage (Bode and Dong, 2007; Zhang et al., 2019). In the control HCT116 cells, the proportions of cells in the G1 phase, S phase, and G2/M phase were

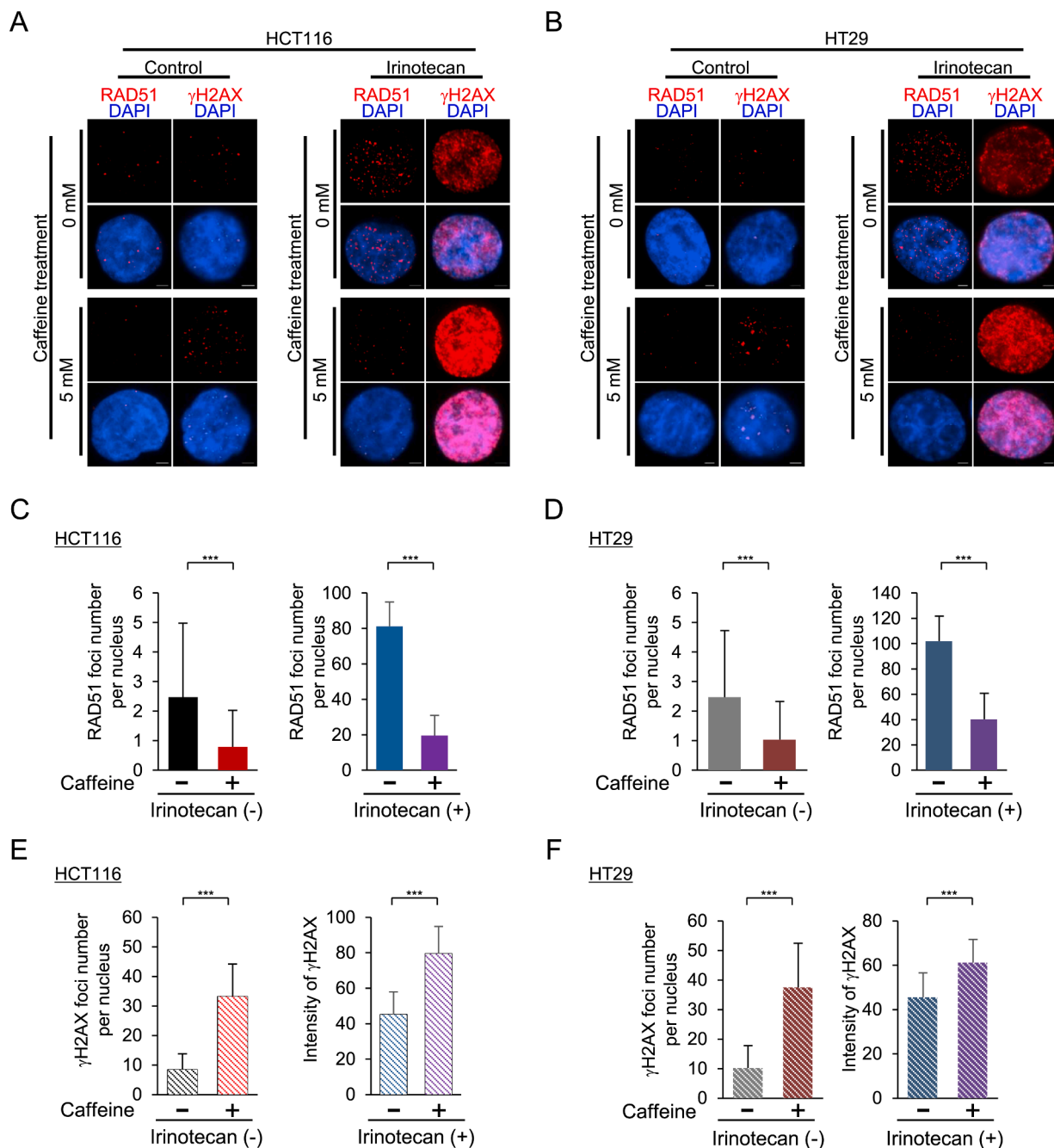


**Fig. 3.** Remaining DNA lesions induced by displacement of RAD51 from DNA breaks. (A, B) Representative images of focus formation of RAD51 and  $\gamma$ H2AX. HCT116 cell line (A) and HT29 cell line (B) were stained with RAD51- and  $\gamma$ H2AX-specific antibodies. Scale bars = 2.5  $\mu$ m. (C, D) Number of formed RAD51 foci. Focus formation of the RAD51 factor was quantified in the HCT116 cell line (C) and HT29 cell line (D) under each condition: control, caffeine, irinotecan, and caffeine + irinotecan. The three experiments were performed independently ( $n = 60$ ). The error bars indicate the mean  $\pm$  SD. (E, F) Quantification of  $\gamma$ H2AX focus formation and signal intensity. The number of foci and intensity of  $\gamma$ H2AX were quantified in both the HCT116 cells (E) and HT29 cells (F). The error bars denote the mean  $\pm$  SD, and the experiments were independently conducted three times ( $n = 60$ ).

approximately  $36.05 \pm 1.93\%$ ,  $31.00 \pm 5.08\%$ , and  $32.94 \pm 3.15\%$ , respectively. Upon caffeine treatment in HCT116 cells, while the proportion of cells in the G2/M phase increased compared to the control, reaching up to  $43.67 \pm 1.33\%$ , the percentage of cells in the G1 phase and S phase decreased to  $29.34 \pm 2.21\%$  and  $26.98 \pm 3.32\%$ , respectively (Fig. 4A and C). In HT29 cells, the proportion of cells in the G1 phase, S phase, and G2 phase was  $43.96 \pm 0.94\%$ ,  $37.70 \pm 4.15\%$ , and  $18.35 \pm 5.05\%$ , respectively. Upon caffeine treatment, the ratio of cells in the S phase increased approximately 1.4-fold compared to the control cells ( $50.9 \pm 13.8\%$  in the caffeine-treated HT29 cell line). Meanwhile,

the proportions of cells in the G1 and G2 phases decreased compared to normal HT29 cells. Specifically, the proportion of cells in the G1 phase was  $34.94 \pm 7.55\%$ , and that of the cells in the G2 phase was  $14.19 \pm 6.41\%$ . These results indicate that caffeine treatment alters cell cycle of CRC cells although the effects of caffeine treatment on the cell cycle vary among different CRC cell lines. When irinotecan was added, most of the HT29 cells ( $62.78\%$ ) were arrested in the S phase. Furthermore, HT29 cells treated with both irinotecan + caffeine were also arrested at the S phase, with proportions of up to  $75.99 \pm 12.37\%$ . In contrast, the percentage of G1 phase HT29 cells in the irinotecan-treated group was

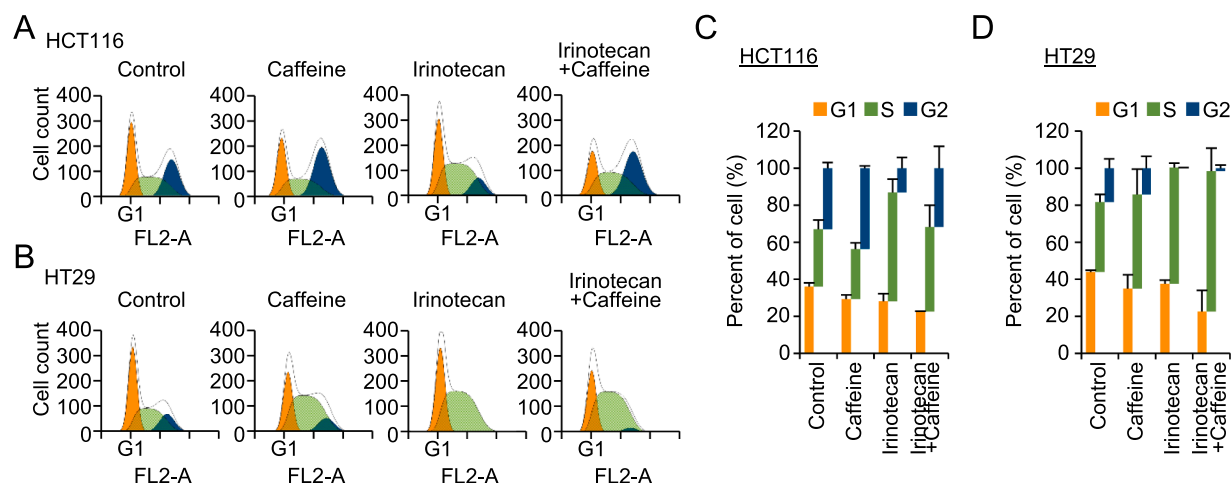


**Fig. 4.** Effects of irinotecan and caffeine on cell cycle pattern. (A)–(D) Cell cycle pattern in HCT116 cells and HT29 cells. Cell cycle progression analysis was performed for both colorectal cell lines, HCT116 (A) and HT29 (B), under each experimental condition. The percentage of cells in each cell cycle phase was measured for both the HCT116 cell line (C) and HT29 cell line (D). The graphs indicate the average, and the error bars represent the standard deviation ( $n = 3$ ).

37.55 ± 2.0%, whereas the group treated with irinotecan + caffeine exhibited a proportion of 22.60 ± 11.40% (Fig. 4B and D). Furthermore, the proportion of G2 phase HT29 cells in the irinotecan or irinotecan + caffeine treatment groups was dramatically decreased, with proportions as low as 0% in the irinotecan-treated HT29 cells and 1.41% in the HT29 cells treated with irinotecan + caffeine. HCT116 cells with DNA damage induced by irinotecan exhibited a larger proportion of S-phase cells, and similarly, Topo I-inhibited HT29 cells with the treatment of irinotecan also had a higher S-phase ratio. In HCT116 cells treated with irinotecan, approximately 28.12% of the cells were in the G1 phase, 58.83% in the S phase, and 13.05% in the G2/M phase (Fig. 4A and C). Furthermore, the cell line treated with both irinotecan and caffeine exhibited a marked effect on the S-phase ratio. In HCT116 cells treated with both irinotecan and caffeine, the proportions of G1-phase, S-phase, and G2/M-phase cells were 22.58 ± 0.15%, 45.75 ± 11.71%, and 31.68 ± 11.82%, respectively (Fig. 4A and C). These results demonstrate that irinotecan blocks cell cycle progression at the S phase, suggesting that this drug could affect DNA replication because Topo I is essential for DNA replication during the S phase by inhibiting the formation of supercoiled DNA to maintain genomic stability.

Fiber assays were also conducted to confirm the relationship between DNA replication and exposure to irinotecan and caffeine. Fiber

length was shortened in the CRC cells treated with the DNA damage agents (Fig. 5A–D). In HCT116 cells, the fiber length of the control cells was approximately 9.0 ± 1.0 μm, whereas those of the caffeine, irinotecan, and irinotecan + caffeine treatment groups were 7.2 ± 1.1 μm, 6.5 ± 1.0 μm, and 5.5 ± 0.6 μm, respectively (Fig. 5A and B). Similarly, the length of DNA replication in the control HT29 cells was 10.4 ± 1.4 μm, whereas those of the caffeine, irinotecan, and irinotecan + caffeine treatment groups were 8.2 ± 1.6 μm, 7.1 ± 1.1 μm, and 6.3 ± 0.9 μm, respectively (Fig. 5C and D). Interestingly, DNA replication in both cell lines treated with the combination of irinotecan and caffeine was significantly stalled (Fig. 5A–D). These results demonstrate that while DNA replication efficiency was substantially reduced by irinotecan or caffeine treatment alone, the combination of both irinotecan and caffeine synergistically decreased DNA synthesis via the accumulation of DNA gaps.

#### Irinotecan enhances caffeine-induced DNA fragmentation

Our findings demonstrated that although the DNA damage effects of caffeine-only treatment were generally not dramatic, caffeine synergistically promoted the DNA damage effects when combined with the DNA damage drug irinotecan. Therefore, we next sought to evaluate the

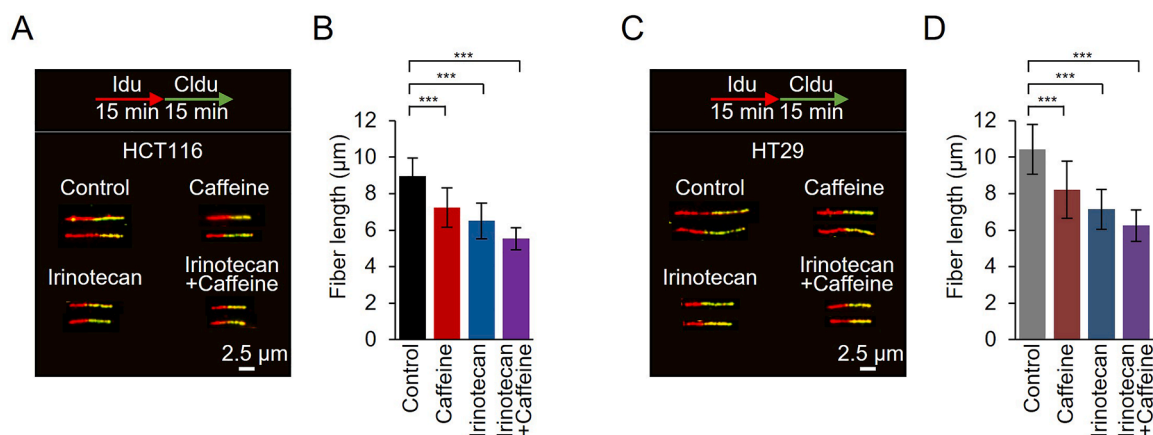


**Fig. 5.** Interruption of DNA replication progress in DNA damaged CRC cells (A) and (C) Labeling of DNA replication. The DNA fiber assay schematic is shown at the top. DNA synthesis was labeled with IdU for 15 min and CldU for 15 min in HCT116 cells (A) and HT29 cells (C). IdU was labeled with red color, and CldU was stained with green color. (B, D) Quantification of newly synthesized DNA. The length of the IdU and CldU tracks was measured in both the HCT116 (B) and HT29 (D) colorectal cancer cell lines. Three independent experiments were performed, and the error bars indicate the mean ± SD ( $n = 60$  for each condition, scale bar = 2.5 μm).

effects of irinotecan and caffeine co-treatment on DNA fragmentation in HCT116 and HT29 cells using the comet assay. The tail moment of the control HCT116 cells was  $5.6 \pm 1.7$ , whereas that of the irinotecan and irinotecan + caffeine-treated HCT116 cells was approximately  $15.8 \pm 3.7$  and  $21.5 \pm 4.3$ , respectively (Fig. 6A and B). The tail moment of HCT116 cells with DNA damaged by irinotecan was significantly (2.82-fold) larger than that of the control HCT116 cells. Furthermore, the

irinotecan + caffeine treatment induced even more DNA fragmentation (3.85-fold compared to the control). Similarly, in HT29 cells, irinotecan resulted in severe DNA fragmentation, with the tail moment increased by 211.2% compared to the control. Specifically, the tail moment of the control HT29 cells was  $10.3 \pm 3.2$ , whereas that of the irinotecan-treated HT29 cells was  $21.8 \pm 4.5$ . Moreover, both irinotecan and caffeine induced higher cell mortality by substantially increasing DNA

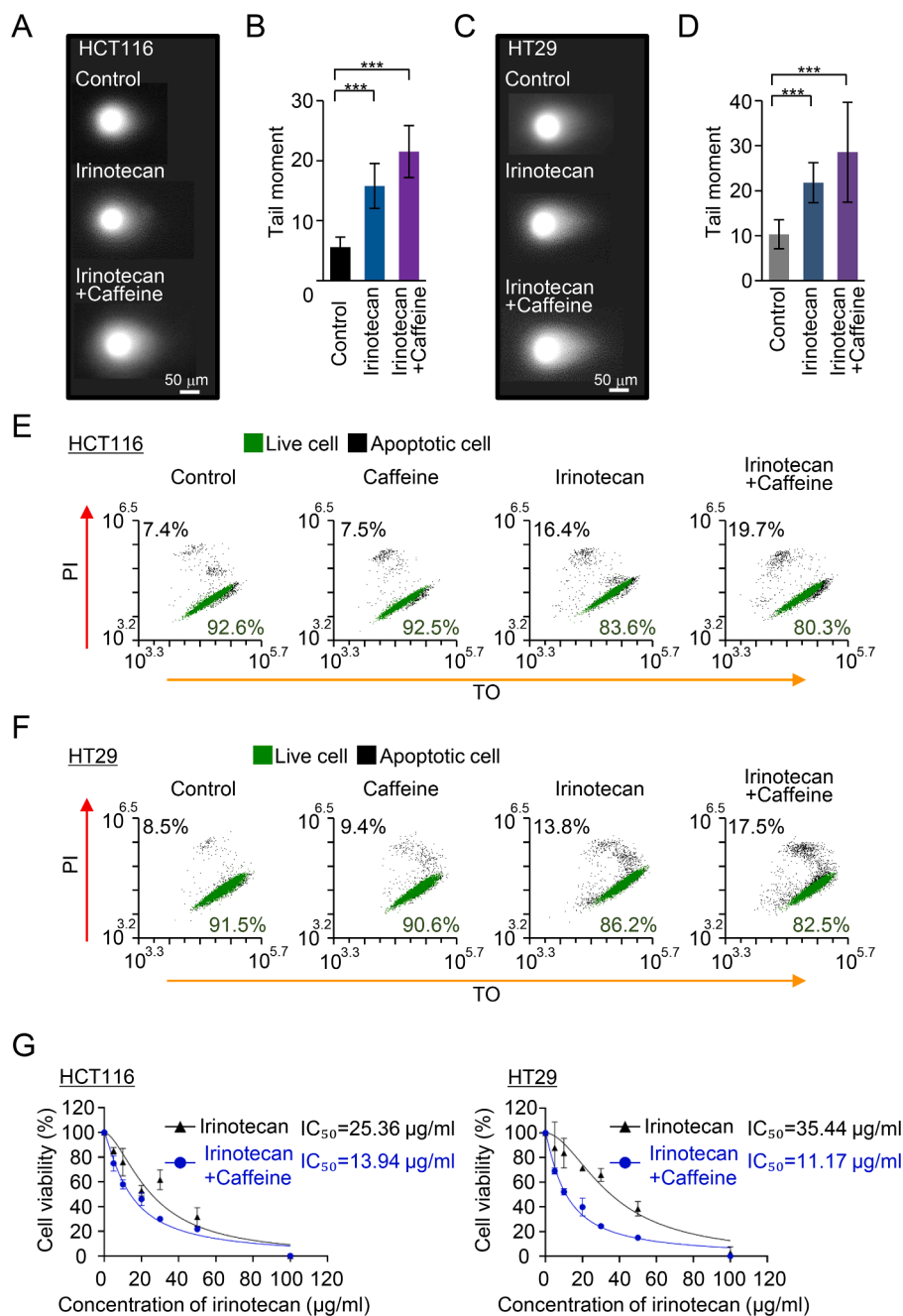


**Fig. 6.** Caffeine treatment stimulates the occurrence of DNA breaks and cell death. (A–D) Analysis of DNA fragmentation via the comet assay. (A, C) Representative images of DNA breaks. HCT116 (A) and HT29 cells (C) were treated with irinotecan, caffeine, or irinotecan + caffeine. A total of 40 cells were quantified under each experimental condition using the Casp software (1.2.3beta2). (B, D) Measurement of tail moments. The tail length was calculated with the following formula: tail length × % of DNA in the tail. All experiments were performed in triplicate (i.e., three independent experiments). The graphs indicate the average ± SD. (E, F) Analysis of cell viability of CRC cells using FACS. HCT116 cells and HT29 cells were incubated under each condition: caffeine, irinotecan, and irinotecan + caffeine. For cell viability analysis, the cells were stained with thiazole orange (TO) and propidium iodide (PI). The black and green dots indicate the apoptotic and live cells, respectively. (G) Analysis of the dose-dependent inhibitory effects of irinotecan via the WST-8 assay. In HCT116 cells (Left panel) and HT29 cells (Right panel), different concentrations of irinotecan were evaluated (0, 5, 10, 20, 30, 50, and 100 µg/ml). The black line indicates cell viability under treatment with irinotecan at various concentrations, whereas the blue line graph shows cell viability at various concentrations of irinotecan in CRC cells treated with 5 mM caffeine. The IC<sub>50</sub> value was calculated using the GraphPad Prism 9 software. Error bars indicate the mean ± SD (*n* = 3).

fragmentation (2.77-fold compared to the control) (Fig. 6C and D). These results suggest that caffeine dramatically enhances the effects of irinotecan on DNA damage.

#### Caffeine promotes cell death by enhancing the cytotoxicity of irinotecan

Our findings demonstrated that interrupting RAD51 function inhibited DNA repair, leading to DNA fragmentation and an accumulation of DNA breaks due to improper DNA repair. Cell viability rates were evaluated in both the HCT116 and HT29 CRC cell lines under three experimental conditions (caffeine, irinotecan, and irinotecan + caffeine). In the HCT116 cell line, the proportion of apoptotic cells was similar after caffeine treatment (7.4% in control cells and 7.5% in caffeine-treated cells). In contrast, in Topo I-inhibited HCT116 cells with

the treatment of irinotecan, the proportion of apoptotic cells was 16.4% (Fig. 6E). Furthermore, the percentage of apoptotic HCT116 cells treated with both irinotecan and caffeine increased to 19.7%. Likewise, in the HT29 cells, the proportion of live caffeine-treated cells was similar to that of the control group (i.e., 91.5% in the control group vs. 90.6% in the caffeine-treated group). However, there was a significant increase in apoptotic HT29 cells in the irinotecan-treated group (13.8%), and the irinotecan + caffeine treatment group exhibited an even higher proportion of 17.5% (Fig. 6F). Additionally, in irinotecan-treated HCT116 cells, the  $IC_{50}$  value was 25.36  $\mu\text{g}/\text{ml}$ , whereas in both irinotecan and caffeine-treated HCT116 cells, the  $IC_{50}$  value was 13.94  $\mu\text{g}/\text{ml}$ . Similarly, in irinotecan-treated HT29 cells, the  $IC_{50}$  value was 35.44  $\mu\text{g}/\text{ml}$ , and in HT29 cells treated with both drugs, the  $IC_{50}$  value was 11.17  $\mu\text{g}/\text{ml}$  (Fig. 6G). The half inhibition concentration was much lower in CRC

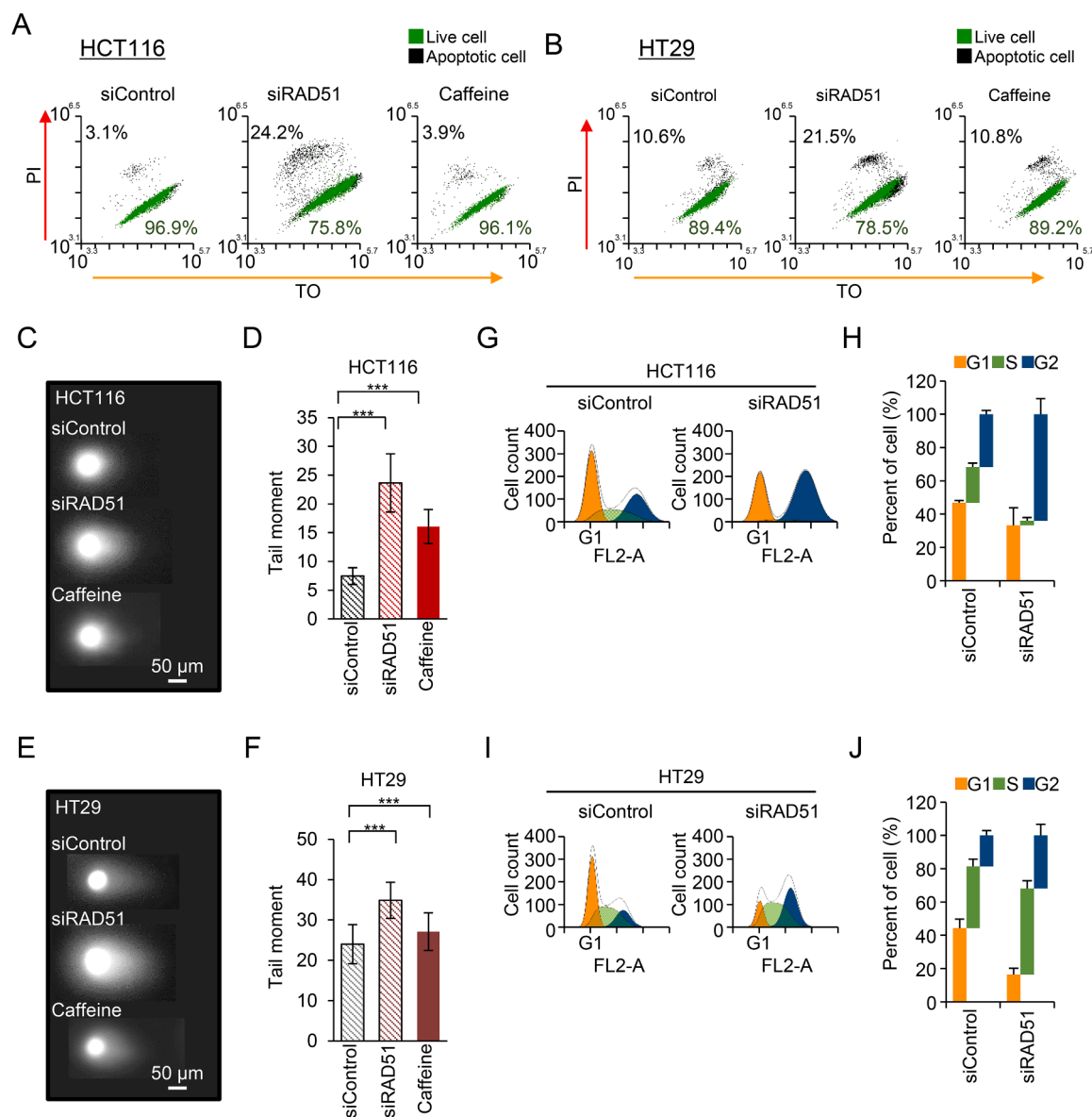


**Fig. 7.** Improvement of stalled DNA replication and generation of DNA breaks by RAD51 depletion. (A, B) Cell viability analysis in colorectal cancer cells with siRAD51 and caffeine. Cell survival was analyzed in the HCT116 cell line (A) and HT29 cell line (B) treated with siRNA against RAD51 for 48 h or caffeine for 4 h. RAD51-depleted cells or control cells were stained with TO and PI. (C–F) Comet assay for analysis of DNA breaks. The RAD51-depleted and caffeine-treated HCT116 cell line (C) and HT29 cell line (E) exhibited the characteristic hallmarks of DNA breaks, as demonstrated by the comet assay. DNA breaks were also quantified by calculating tail moment in HCT116 cells (D) and HT29 cells (F). The tail moment was calculated for 40 cells, and the graphs indicate the mean  $\pm$  SD. Three assays were performed independently. (G–J) Analysis of cell cycle progression. In RAD51-depleted HCT116 cells (G, H) and HT29 cells (I, J), cell cycle analysis was carried out using a flow cytometer (FACSCalibur, Becton Dickinson). The pattern of the cell cycle was analyzed with the ModFit software (H, J). Three independent analyses were performed (mean  $\pm$  SD).

cells treated with irinotecan + caffeine than in those treated with irinotecan only. Moreover, 5-fluorouracil (5-FU) treatment, which is commonly used for colon cancer therapy through inhibiting thymidylate synthase, along with caffeine, induced a reduction in the IC<sub>50</sub> value compared to treatment with only 5-FU (Fig. S1A) (Longley et al., 2003; Cho et al., 2020). In HCT116 cells, the 5-FU-only treatment had an IC<sub>50</sub> value of 11.47 μM, whereas the 5-FU + caffeine treatment had a value of 4.192 μM. Similarly, in HT29 cells, the IC<sub>50</sub> values for the aforementioned treatments were 13.06 and 2.816 μM, respectively (Fig. S1A). In addition, solvents, DMSO and PBS, had no significant gap of cell viability between only DMSO treated cells and DMSO and PBS treated cells (Fig. S1B and C). These results demonstrate that existing anticancer drugs could affect the viability of CRC cells, and this effect was synergistically enhanced by co-exposure with caffeine.

#### *Disruption of RAD51 function induces cell death by inhibiting the mechanisms required to maintain genome integrity*

Caffeine hinders the function of RAD51, one of the main factors in HR, by evicting it from ssDNA, leading to incomplete DNA repair and replication. To further compare the effects of disrupting DNA repair progression between caffeine-treated cells and RAD51-depleted cells, RAD51 was knocked down in both the HCT116 and HT29 cell lines using RAD51-specific siRNA. The depletion efficiency was approximately 90% in both cell lines (Fig. S2). In the caffeine-treated HCT116 cells, the proportion of live cells was approximately 96.1%, whereas the survival of RAD51-depleted HCT116 cells was approximately 75.8% (Fig. 7A). Additionally, the survival of caffeine-treated HT29 cells was 89.2%, whereas that of the RAD51-depleted HT29 cells was 78.5% (Fig. 7B). However, in both caffeine-treated cell lines, the cell survival rate was similar to that of the control. Specifically, the proportions of live caffeine-treated HCT116 and HT29 cells were 3.9 and 10.8%, respectively (Fig. 7A and B). RAD51 depletion had a much stronger effect on cell survival than caffeine treatment by directly disrupting DNA replication or the progression of repair mechanisms, leading to cell death. Furthermore, we assessed DNA fragmentation under each experimental condition using the comet assay (Fig. 7C–F). In the HCT116 cells, the DNA fragmentation of the RAD51-depleted cells was more than 3.2-fold higher than that of the siControl cells (Fig. 7C and D). Similarly, the caffeine-treated HCT116 cells exhibited approximately 2.2 times more DNA fragmentation than the control HCT116 cells (Fig. 7C and D). The tail moment of the siControl HT29 cells was approximately 24.0 ± 4.9, whereas that of the RAD51-depleted HT29 cells was approximately 34.9 ± 4.5, representing a 1.5-fold increase compared to the control HT29 cells (Fig. 7E and F). In contrast, the tail moment of the caffeine-treated HT29 cells was approximately 27.1 ± 4.7 (Fig. 7E and F). Collectively, our results demonstrate that RAD51 depletion increases the tail length of both cell lines, suggesting that the absence of RAD51 leads to DNA fragmentation, resulting in cell death. Caffeine also induces a substantial increase in DNA fragmentation.

Furthermore, our findings also demonstrated that RAD51 depletion significantly altered the cell cycle progression of CRC cells. In the siControl HCT116 cells, the proportion of G1-phase, S-phase, and G2/M-phase cells were approximately 46.80, 21.46 and 31.74%, respectively (Fig. 7G, H). However, in RAD51-depleted HCT116 cells, the G1 phase and S phase ratios were dramatically decreased by approximately 30 and 88%, respectively (Fig. 7G and H), whereas the proportion of cells in the G2/M phase increased to 29% of the total cells (Fig. 7G and H). Likewise, in RAD51-depleted HT29 cells, there was an elevation in the percentage of cells in the G2/M phase, accompanied by a reduction in the portion of cells in the G1 phase. In contrast to HCT116 case, the RAD51-depleted HT29 cells showed a noticeable increase in cells within the S phase, with a comparison of 37.16% in control cells to 51.77% in RAD51-depleted cells (Fig. 7I and J). During the S-phase, HR (i.e., a key DNA repair mechanism) begins to fill the DNA gaps that occur during DNA replication. RAD51 is one of the most important factors in HR, and our

findings suggested that this recombinase is essential during the S-phase. Therefore, the absence of RAD51 substantially affected cell cycle progression. Taken together, our findings suggested that irinotecan and caffeine co-treatment could enhance cancer cell apoptosis by inhibiting RAD51 functions.

## Discussion

The function and role of the RAD51-mediated DNA repair mechanism are conserved in most eukaryote organisms. Additionally, this is a key process that suppresses genetic mutation and promotes cell proliferation. Changes in the RAD51-mediated DNA repair mechanism can thus cause cell mutation and various physiological changes within cells (Aguilera and Gómez-González, 2008; Helleday et al., 2008). The DNA repair pathway in CRC cells is highly activated, making the suppression of DNA repair a promising cancer treatment strategy (Vispé et al., 1998; Zhou et al., 2020; Schild and Wiese, 2010). Inhibiting DNA repair pathways in cancer cells can enhance the effectiveness of chemotherapy and radiation therapy, both of which induce DNA damage, leading to a greater accumulation of DNA damage and ultimately resulting in cell death. Our findings suggest that irinotecan and caffeine co-treatment can enhance CRC cell death by inhibiting proper DNA repair and disrupting rapid cell cycle progression. Cancer cells exhibit abnormally fast proliferation, thus limiting DNA repair time (Manic et al., 2021; Tennstedt et al., 2013; Grundy et al., 2020). Therefore, DNA repair genes are highly expressed in cancer cells to compensate for this time limitation, enabling the repair of DNA damage caused by DNA replication or external/internal factors. RAD51, a major contributor to DNA repair, facilitates DNA replication or repair processes to maintain genomic stability (Choi et al., 2017b). RAD51 is abundantly expressed in many human cancers such as CRC, breast cancer, and pancreatic cancer, thus contributing to resistance to cancer therapy (Pommier et al., 2022). Therefore, this factor is a promising target for the treatment of malignant tumors via chemotherapy (Pommier et al., 2022). Irinotecan is a promising Topo I-targeting drug that is often used as a first-line treatment for metastatic CRC cells. Topo I is highly expressed in CRC cells compared to normal colon cells (Rømer et al., 2012). This enzyme is ubiquitous and plays an essential role in many cellular metabolic processes, including replication, recombination, and transcription (Morham et al., 1996). Its main function is to transiently cleave and rejoin one strand of the DNA duplex, thereby relaxing supercoiled DNA. Topo I-deficient mice and fruit flies with disrupted Topo I function fail to develop during embryogenesis, which highlights the significance of this enzyme during early development (Gemkow et al., 2001; Matsuoka et al., 2007). Therefore, the Topo I enzyme holds great potential as an anticancer therapy target. Irinotecan, a semisynthetic derivative of the plant alkaloid camptothecin, binds to Top1cc, which serves as the interface between topoisomerase and DNA. In turn, irinotecan can lead to the accumulation of Top1cc, thereby inducing the occurrence of DSBs. Therefore, this drug not only causes DNA breaks but also leads to cell death.

Our study sought to assess whether co-treatment with irinotecan and caffeine could lead to the accumulation of DNA breaks, resulting in cancer cell death. When DNA breaks occur due to either endogenous or exogenous factors, the histone variant H2AX is rapidly phosphorylated at serine 139 by serine-threonine kinases such as ATM, ATR, and DNA-PK. This phosphorylated form, known as γH2AX, plays a critical role in the DNA damage response, activating the DNA repair system (Choi et al., 2017a; Yoon et al., 2018). The Mre11-Rad50-NBS1 complex recognizes DNA breaks, triggering the activation of ATM and subsequent DNA repair pathways (Li and Heyer, 2008; Krejci et al., 2012). Exonuclease I generates single-strand DNA (ssDNA) by trimming the broken DNA strand (Li and Heyer, 2008; Krejci et al., 2012). Following DSB end resection, the 3' overhang of the DSB is exposed and replication protein A (RPA) binds to the ssDNA to prevent secondary structure formation (Li and Heyer, 2008; Bhat and Cortez, 2018). Afterward, RAD51

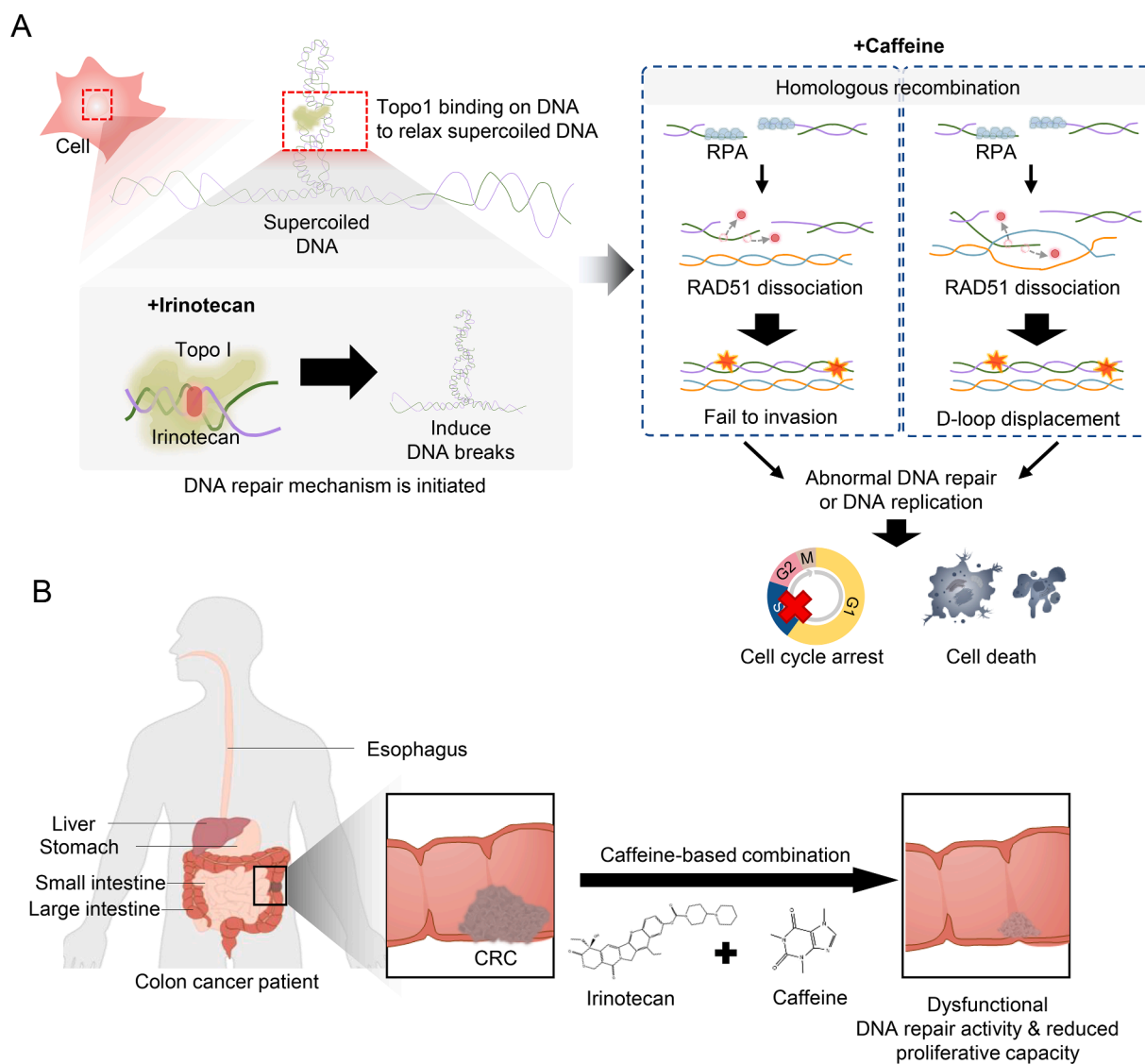


**Fig. 8.** Proposed model of the synergistic effects of caffeine co-administration. (A) Molecular mechanism of synergistic effects. Supercoiled DNA can form during DNA replication or transcription. Topo I binds to supercoiled DNA to relax it and forms a phosphodiester bond between the broken DNA end and tyrosine 723 residue in Topo I, known as Top1cc. In the presence of irinotecan, Top1cc is trapped by the camptothecin derivative, leading to the accumulation of DNA breaks. Homologous recombination, a crucial DNA repair process, is then initiated to repair DNA lesions induced by irinotecan. During DNA repair, caffeine could hinder the completion of the repair process by inhibiting RAD51, a key factor in the repair system, ultimately inducing cell death. Colorectal cancer cells would be more susceptible to cell death in the presence of both irinotecan and caffeine compared to only the presence of irinotecan. (B) Model of the possible efficiency of the combination therapy. CRC cells are sensitive to irinotecan and caffeine co-treatment. Both drugs work synergistically, with irinotecan inducing DNA breaks and caffeine inhibiting proper DNA repair.

localizes to the break sites coated with RPA, a process facilitated by BRCA2, leading to the formation of the nucleoprotein filament known as the presynaptic filament (Krejci et al., 2012). The ssDNA-RAD51 filament then searches for homology and invades the homologous template to form D-loop (displacement-loop) structures. DNA synthesis follows D-loop formation, and the synthesized DNA is captured to form Holliday junctions. The structure is eventually resolved, and the gaps are filled, thus completing the repair system to mend the DNA breaks (Li and Heyer, 2008; Krejci et al., 2012). Additionally, RAD51 participates not only in DNA repair but also in DNA replication. This phenomenon is known as replication fork protection and prevents the degradation of stalled replication forks (Bhat and Cortez, 2018; Bhowmick et al., 2022). In our study, the protein expression of RAD51 was found to be similar in both caffeine- and irinotecan-treated CRC cells (Fig. 2E and F). Moreover, in HCT116 and HT29 cells treated with both irinotecan and caffeine, the expression level of RAD51 tended to be similar regardless of

anticancer drug treatment (Fig. 2E and F). However, the level of  $\gamma$ H2AX, a marker for DSBs, showed a significant increase in CRC cells treated with both irinotecan and caffeine (Fig. 3). In contrast, caffeine treatment resulted in a distinct RAD51 focus formation pattern compared to that of  $\gamma$ H2AX focus formation. In both caffeine- and irinotecan + caffeine-treated CRC cells, RAD51 foci number decreased by more than 60% in both cell lines (Fig. 3). The inhibition of RAD51 resulted in improper DNA repair and a significant increase in the occurrence of DSBs. Both topoisomerase and RAD51 play crucial roles in DNA replication, and therefore changing their expression resulted in substantial changes in DNA replication patterns. Therefore, irinotecan and caffeine co-treatment could alter the cell cycle pattern in CRC cells. Additionally, the length of newly synthesized DNA in CRC cells treated with both drugs was much shorter than that of the cells treated with only caffeine or irinotecan. Furthermore, the accumulation of DNA breaks slowed down the DNA replication speed. Various cellular metabolic processes

including DNA repair, DNA replication, and programmed cell death could be impaired by caffeine (Tsabar et al., 2015; Zelensky et al., 2013; Bode and Dong, 2007). Caffeine has been reported to (i) suppress RAD51 localization onto DNA break sites, (ii) inhibit the function of several kinases such as ATM and ATR, leading to arrest at the G2/M phase to activate cell cycle checkpoints, and (iii) affect the resection of DSB ends by degradation of resection factors (Tsabar et al., 2015; Zelensky et al., 2013; Bode and Dong, 2007). Similarly, another study demonstrated that caffeine inhibits DNA repair, which negatively affects genomic stability, leading to the accumulation of DNA breaks during DNA repair or replication. On the other hand, irinotecan, a camptothecin derivative, has shown great promise as an anti-cancer treatment. This is because camptothecin targets only Topo I, penetrates cells rapidly after treatment, and binds reversibly to Top1cc (Pommier, 2006). This trapping of Top1cc by irinotecan leads to its accumulation in cells, inhibiting DNA replication and transcription machinery, activating cell cycle arrest, and ultimately inducing cell death (Pommier, 2006; Pommier et al., 2010; Thomas and Pommier 2019; Strumberg et al., 2000).

Co-treatment with irinotecan and caffeine induced severe DNA fragmentation and led to cell apoptosis (Fig. 6). In addition, co-treatment of 5-FU which is widely used for chemotherapy for cancer, especially colorectal cancer, and caffeine led to reduction of IC<sub>50</sub> (Fig. S1A) (Longley et al., 2003). 5-FU, an uracil analogue, has a fluorine atom at the C5 in place of hydrogen, inducing interrupting thymidylate synthase (TS) which converts from deoxyuridine monophosphate (dUMP) to deoxythymidine monophosphate (dTMP) and is important to DNA synthesis (Longley et al., 2003). 5-FU is converted to fluorodeoxyuridine monophosphate (FdUMP) which is an active metabolite, in the body and FdUMP binds to the nucleotide-binding site of TS, inducing formation of ternary complex with 5,10-methylene tetrahydrofolate (CH<sub>2</sub>THF) (Garg et al., 2010; Longley et al., 2003). The complex consisting of TS, FdUMP and CH<sub>2</sub>THF induces imbalance of deoxythymidine triphosphate (dNTP) pool by inhibiting binding dUMP which could be converted to dTMP by TS (Longley et al., 2003). The imbalance of dNTP pool resulted from 5-FU could induce DNA breaks and, consequently, DNA repair process is initiated to repair the DNA lesions (Adamsen et al., 2011; Matuo et al., 2009; Nakagawa et al., 2014). RAD51 is known for its key role in maintaining genome integrity. Therefore, the depletion or knockout of RAD51 in many species is lethal. In zebrafish, the loss of RAD51 leads to Fanconi anemia-like symptoms (Botthof et al., 2017), whereas abnormal spermatogenesis and embryo lethality were reported in RAD51-depleted mice (Dai et al., 2017; Tsuzuki et al., 1996). In RAD51-depleted colorectal cells, the occurrence of DNA breaks was dramatically increased (Fig. 7C–F) and cell viability was significantly reduced (Fig. 7A and B). Changes in the cell cycle lead to the activation of the DNA damage checkpoint system to fix the breaks. Therefore, inhibition of RAD51 function caused an accumulation of DNA fragmentation, ultimately leading to cell death. Several drugs targeting various molecules have been developed. Particularly, a treatment for CRC involving DNA replication and synthesis was developed and its therapeutic effects were enhanced through synergistic interaction with other compounds. Moreover, drug development targeting HR factors, which are expected to have a very strong therapeutic effect, may be necessary to develop novel cancer treatments.

The results of our study demonstrated that caffeine can significantly enhance the chemosensitivity of CRC cells to irinotecan, providing evidence for the potential of caffeine as an adjuvant therapy in the treatment of CRC (Fig. 8A). Our findings thus contribute to the growing body of evidence on the therapeutic benefits of caffeine in cancer treatment and highlights the need for further research to validate our results. HR factors such as RAD51, BRCA1/2, and RAD52, which are overexpressed by CRC cells, are also involved in DNA replication. Exploring this phenomenon may provide the necessary insights to reduce the activity of DNA repair and replication efficiency for CRC treatment. Furthermore, in various cancer types, RAD51 expression levels were much higher than in normal cells, leading to increased resistance to chemotherapy or

radiation therapy (Gachechiladze et al., 2017; Wang et al., 2022). Here, we found that caffeine had little effect on DNA breaks or cell viability, although it inhibited RAD51 focus formation by displacing the RAD51 factor from DNA lesions. On the other hand, caffeine could improve the effects of the traditional drug for colorectal cancer therapy, irinotecan. Therefore, the results of our *in vitro* analyses using two types of colorectal cancer cells (HCT116 and HT29) highlight the potential applicability of caffeine as a potentiator of cancer therapy. However, *in vivo* experiments using mouse cancer models must still be conducted to optimize drug concentrations and assess their applicability to cancer patients.

## Conclusion

Targeting RAD51 with specific inhibitors or other therapeutic strategies could potentially reduce the ability of CRC cells to repair DNA damage, leading to cell death and inhibition of cell proliferation (Fig. 8). However, any RAD51-targeted therapy would need to be carefully designed to minimize toxicity to normal cells while effectively inhibiting the proliferation of CRC cells. Furthermore, our findings demonstrated that caffeine suppresses the growth of CRC cells by targeting RAD51 during DNA repair and HR, and therefore additional research is needed to identify the optimal methods to utilize and administer caffeine to cancer patients, as well as to determine the safety and potential side effects of caffeine as a cancer therapy.

## Funding

This work was supported by grants to K.P.K. from the National Research Foundation of Korea (NRF) grant funded by the Korean government (MSIT) (RS-2023-00208191) and the Kun-hee Lee Seoul National University Hospital Child Cancer & Rare Disease Project, Republic of Korea (22B-001-0500).

## CRediT authorship contribution statement

**Seobin Yoon:** Conceptualization, Methodology, Validation, Formal analysis, Investigation, Resources, Data curation, Writing – original draft, Writing – review & editing, Visualization, Supervision, Project administration, Funding acquisition. **Bum-Kyu Lee:** Conceptualization, Writing – original draft, Writing – review & editing. **Keun Pil Kim:** Conceptualization, Methodology, Formal analysis, Writing – original draft, Writing – review & editing, Supervision, Project administration, Funding acquisition.

## Declaration of Competing Interest

The authors declare that they have no known competing financial interests or personal relationships that could have appeared to influence the work reported in this paper.

## Supplementary materials

Supplementary material associated with this article can be found, in the online version, at [doi:10.1016/j.phymed.2023.155120](https://doi.org/10.1016/j.phymed.2023.155120).

## References

- Adamsen, B.L., Kravik, K.L., De Angels, P.M., 2011. DNA damage signaling in response to 5-fluorouracil in three colorectal cancer cell lines with different mismatch repair and TP53 status. *Int. J. Oncol.* 39, 673–682.
- Aguilera, A., Gómez-González, B., 2008. Genome instability: a mechanistic view of its causes and consequences. *Nat. Rev. Genet.* 9, 204–217.
- Bhat, K.P., Cortez, D., 2018. RPA and RAD51: fork reversal, fork protection, and genome stability. *Nat. Struct. Mol. Biol.* 25, 446–453.
- Bhowmick, R., Lerdrup, M., Gadi, S.A., Rossetti, G.G., Singh, M.I., Liu, Y., Halazonetis, T. D., Hickson, I.D., 2022. RAD51 protects human cells from transcription-replication conflicts. *Mol. Cell.* 82, 3366–3381.

- Bode, A.M., Dong, Z., 2007. The enigmatic effects of caffeine in cell cycle and cancer. *Cancer Lett.* 247, 26–39.
- Bothof, J.G., Bielczyk-Maczyńska, E., Ferreira, L., Cvejic, A., 2017. Loss of the homologous recombination gene rad51 leads to Fanconi anemia-like symptoms in zebrafish. In: *Proceedings of the National Academy of Sciences of the United States of America*, 114, pp. E4452–E4461.
- Champoux, J.J., 1981. DNA is linked to the rat liver DNA nicking-closing enzyme by a phosphodiester bond to tyrosine. *J. Biol. Chem.* 256, 4805–4809.
- Cho, Y.H., Ro, E.J., Yoon, J.S., Mizutani, T., Kang, D.W., Park, J.C., Kim, T.I., Clevers, H., Choi, K.Y., 2020. 5-FU promotes stemness of colorectal cancer via p53-mediated WNT/β-catenin pathway activation. *Nat. Commun.* 11, 1–13.
- Choi, E.H., Kim, K.P., 2019. E2F1 facilitates DNA break repair by localizing to break sites and enhancing the expression of homologous recombination factors. *Exp. Mol. Med.* 51, 1–12.
- Choi, E.H., Yoon, S., Koh, Y.E., Hong, T.K., Do, J.T., Lee, B.K., Hahn, Y., Kim, K.P., 2022. Meiosis-specific cohesin complexes display essential and distinct roles in mitotic embryonic stem cell chromosomes. *Genome Biol.* 23, 1–31.
- Choi, E.H., Yoon, S., Koh, Y.E., Seo, Y.J., Kim, K.P., 2020. Maintenance of genome integrity and active homologous recombination in embryonic stem cells. *Exp. Mol. Med.* 52, 1220–1229.
- Choi, E.H., Yoon, S., Park, K.S., Kim, K.P., 2017a. The homologous recombination machinery orchestrates post-replication DNA repair during self-renewal of mouse embryonic stem cells. *Sci. Rep.* 7, 11610.
- Choi, E.H., Yoon, S., Hahn, Y., Kim, K.P., 2017b. Cellular dynamics of Rad51 and Rad54 in response to postreplicative stress and DNA damage in HeLa cells. *Mol. Cells* 40, 143–150.
- Choi, E.H., Yoon, S., Kim, K.P., 2018. Combined ectopic expression of homologous recombination factors promotes embryonic stem cell differentiation. *Mol. Ther.* 26, 1154–1165.
- Cremolini, C., Schirripa, M., Antoniotti, C., Moretto, R., Salvatore, L., Masi, G., Falcone, A., Loupakis, F., 2015. First-line chemotherapy for mCRC—a review and evidence-based algorithm. *Nat. Rev. Clin. Oncol.* 12, 607–619.
- Dai, J., Voloshin, O., Potapova, S., Camerini-Otero, R.D., 2017. Meiotic knockdown and complementation reveals essential role of RAD51 in mouse spermatogenesis. *Cell Rep.* 18, 1383–1394.
- de Castro e Gloria, H., Jesuino Nogueira, L., Bencke Grudzinski, P., da Costa Ghignatti, P. V., Guecheva, T.N., Motta Leguisamo, N., Safi, J., 2021. Olaparib-mediated enhancement of 5-fluorouracil cytotoxicity in mismatch repair deficient colorectal cancer cells. *BMC Cancer* 21, 1–13.
- Feu, S., Unzueta, F., Ercilla, A., Pérez-Venteo, A., Jaumot, M., Agell, N., 2022. RAD51 is a druggable target that sustains replication fork progression upon DNA replication stress. *PLoS One* 17, e0266645.
- Friedberg, E.C., 2001. How nucleotide excision repair protects against cancer. *Nat. Rev. Cancer* 1, 22–33.
- Gachechiladze, M., Skarda, J., Soltermann, A., Joerger, M., 2017. RAD51 as a potential surrogate marker for DNA repair capacity in solid malignancies. *Int. J. Cancer* 141, 1286–1294.
- Garg, D., Henrich, S., Salo-Ahen, O.M.H., Myllykallio, H., Costi, M.P., Wade, R.C., 2010. Novel approaches for targeting thymidylate synthase to overcome the resistance and toxicity of anticancer drugs. *J. Med. Chem.* 53, 6539–6549.
- Gemkow, M.J., Dichter, J., Arndt-Jovin, D.J., 2001. Developmental regulation of DNA-topoisomerases during *Drosophila* embryogenesis. *Exp. Cell Res.* 262, 114–121.
- Grundy, M.K., Buckanovich, R.J., Bernstein, K.A., 2020. Regulation and pharmacological targeting of RAD51 in cancer. *NAR Cancer* 2, zcaa024.
- Han, W., Ming, M., He, Y.Y., 2011. Caffeine promotes ultraviolet B-induced apoptosis in human keratinocytes without complete DNA repair. *J. Biol. Chem.* 286, 22825–22832.
- Hanahan, D., Weinberg, R.A., 2011. Hallmarks of cancer: the next generation. *Cell* 144, 646–674.
- Helleday, T., Petermann, E., Lundin, C., Hodgson, B., Sharma, R.A., 2008. DNA repair pathways as targets for cancer therapy. *Nat. Rev. Cancer* 8, 193–204.
- Kerr, D., 2003. Clinical development of gene therapy for colorectal cancer. *Nat. Rev. Cancer* 3, 615–622.
- Koh, Y.E., Choi, E.H., Kim, J.W., Kim, K.P., 2022. The kleisin subunits of cohesin are involved in the fate determination of embryonic stem cells. *Mol. Cells* 45, 820–832.
- Krejci, L., Altmanova, V., Spirek, M., Zhao, X., 2012. Homologous recombination and its regulation. *Nucleic Acids Res.* 40, 5795–5818.
- Li, L.Y., Guan, Y.D., Chen, X.S., Yang, J.M., Cheng, Y., 2021. DNA repair pathways in cancer therapy and resistance. *Front. Pharmacol.* 11, 1–13.
- Li, X., Heyer, W.D., 2008. Homologous recombination in DNA repair and DNA damage tolerance. *Cell Res.* 18, 99–113.
- Longley, D.B., Harkin, D.P., Johnston, P.G., 2003. 5-Fluorouracil: mechanisms of action and clinical strategies. *Nat. Rev. Cancer* 3, 330–338.
- Manic, G., Musella, M., Corradi, F., Sistigu, A., Vitale, S., Rehim, S.S.A., Mattiello, L., Malacaria, E., Galassi, C., Signore, M., Pallocca, M., Scalera, S., Goeman, F., Nicola, F.D., Guarracino, A., Pennisi, R., Antonangeli, F., Sperati, F., Baiocchi, M., Biffoni, M., Faniulli, M., Maugeri-Saccà, M., Franchitto, A., Pichielli, P., Maria, R.D., Vitale, I., 2021. Control of replication stress and mitosis in colorectal cancer stem cells through the interplay of PARP1, MRE11 and RAD51. *Cell Death Differ.* 28, 2060–2082.
- Matsuoka, S., Ballif, B.A., Smogorzewska, A., McDonald, E.R.III., Hurov, K.E., Luo, J., Bakalarski, C.E., Zhao, Z., Solimini, N., Lerenthal, Y., Shiloh, Y., Gygi, S.P., Elledge, S.J., 2007. ATM and ATR substrate analysis reveals extensive protein networks responsive to DNA damage. *Science* 316, 1160–1166.
- Matuo, R., Sousa, F.G., Escargueil, A.E., Grivicich, I., Garcia-Santos, D., Chies, J.A.B., Safi, J., Larsen, A.K., Henriques, J.A.P., 2009. 5-Fluorouracil and its active metabolite FdUMP cause DNA damage in human SW620 colon adenocarcinoma cell line. *J. Appl. Toxicol.* 29, 308–316.
- Morham, S.G., Kluckman, K.D., Voulomanos, N., Smithies, O., 1996. Targeted disruption of the mouse topoisomerase I gene by camptothecin selection. *Mol. Cell Biol.* 16, 6804–6809.
- Nakagawa, Y., Kajihara, A., Takahashi, A., Kondo, N., Mori, E., Kiritani, T., Ohnishi, T., 2014. The BRCA2 gene is a potential molecular target during 5-fluorouracil therapy in human oral cancer cells. *Oncol. Rep.* 31, 2001–2006.
- Park, S.J., Yoon, S., Choi, E.H., Hyeon, H., Lee, K., Kim, K.P., 2023. Elevated expression of exogenous RAD51 enhances the CRISPR/Cas9-mediated genome editing efficiency. *BMB Rep.* 56, 102–107.
- Pommier, Y., 2006. Topoisomerase I inhibitors: camptothecins and beyond. *Nat. Rev. Cancer* 6, 789–802.
- Pommier, Y., Leo, E., Zhang, H., Marchand, C., 2010. DNA topoisomerases and their poisoning by anticancer and antibacterial drugs. *Chem. Biol.* 17, 421–433.
- Pommier, Y., Nussenzweig, A., Takeda, S., Austin, C., 2022. Human topoisomerases and their roles in genome stability and organization. *Nat. Rev. Mol. Cell Biol.* 23, 407–427.
- Qi, W., Qiao, D., Martinez, J.D., 2022. Caffeine induces TP53-independent G1-phase arrest and apoptosis in human lung tumor cells in a dose-dependent manner. *Radiat. Res.* 157, 166–174.
- Rømer, M.U., Jensen, N.F., Nielsen, S.L., Müller, S., Nielsen, K.V., Nielsen, H.J., Brüner, N., 2012. TOP1 gene copy numbers in colorectal cancer samples and cell lines and their association to in vitro drug sensitivity. *Scand. J. Gastroenterol.* 47, 68–79.
- Schild, D., Wiese, C., 2010. Overexpression of RAD51 suppresses recombination defects: a possible mechanism to reverse genomic instability. *Nucleic Acids Res.* 38, 1061–1070.
- Stenvang, J., Kümler, I., Nygård, S., Smith, D., Nielsen, D., Brüner, N., Moreira, J., 2013. Biomarker-guided repurposing of chemotherapeutic drugs for cancer therapy: a novel strategy in drug development. *Front. Oncol.* 3, 1–9.
- Strumberg, D., Pilon, A.A., Smith, M., Hickey, R., Malkas, L., Pommier, Y., 2000. Conversion of topoisomerase I cleavage complexes on the leading strand of ribosomal DNA into 5'-phosphorylated DNA double-strand breaks by replication runoff. *Mol. Cell Biol.* 20, 3977–3987.
- Tennstedt, P., Fresor, R., Simon, R., Marx, A., Terracciano, L., Petersen, C., Sauter, G., Dikomey, E., Borgmann, K., 2013. RAD51 overexpression is a negative prognostic marker for colorectal adenocarcinoma. *Int. J. Cancer Res.* 132, 2118–2126.
- Thomas, A., Pommier, Y., 2019. Targeting topoisomerase I in the era of precision medicine. *Clin. Cancer Res.* 25, 6581–6589.
- Tsabar, M., Mason, J.M., Chan, Y.L., Bishop, D.K., Haber, J.E., 2015. Caffeine inhibits gene conversion by displacing Rad51 from ssDNA. *Nucleic Acids Res.* 43, 6902–6918.
- Tsuzuki, T., Fujii, Y., Sakumi, K., Tominaga, Y., Nakao, K., Sekiguchi, M., Matsushiro, A., Yoshimura, Y., Morita, T., 1996. Targeted disruption of the Rad51 gene leads to lethality in embryonic mice. In: *Proceedings of the National Academy of Sciences of the United States of America*, 93, pp. 6236–6240.
- Vispé, S., Cazaux, C., Lesca, C., Defais, M., 1998. Overexpression of Rad51 protein stimulates homologous recombination and increases resistance of mammalian cells to ionizing radiation. *Nucleic Acids Res.* 26, 2859–2864.
- Wang, G., Bhoopalan, V., Wang, D., Wang, L., Xu, X., 2015. The effect of caffeine on cisplatin-induced apoptosis of lung cancer cells. *Exp. Hematol. Oncol.* 4, 1–9.
- Wang, Z., Jia, R., Wang, L., Yang, Q., Hu, X., Fu, Q., Zhang, X., Li, W., Ren, Y., 2022. The emerging roles of Rad51 in cancer and its potential as a therapeutic target. *Front. Oncol.* 12, 935593.
- Xie, Y.H., Chen, Y.X., Fang, J.Y., 2020. Comprehensive review of targeted therapy for colorectal cancer. *Signal. Transduct. Target Ther.* 5, 22.
- Xu, Y., Villalona-Calero, M.A., 2002. Irinotecan: mechanisms of tumor resistance and novel strategies for modulating its activity. *Ann. Oncol.* 13, 1841–1851.
- Yoon, S., Choi, E.H., Kim, J.W., Kim, K.P., 2018. Structured illumination microscopy imaging reveals localization of replication protein A between chromosome lateral elements during mammalian meiosis. *Exp. Mol. Med.* 50, 1–12.
- Yoon, S., Choi, E.H., Park, S.J., Kim, K.P., 2023. α-Kleisin subunit of cohesin preserves the genome integrity of embryonic stem cells. *BMB Rep.* 56, 108–113.
- Yoon, S.W., Kim, D.K., Kim, K.P., Park, K.S., 2014. Rad51 regulates cell cycle progression by preserving G2/M transition in mouse embryonic stem cells. *Stem Cells Dev.* 23, 2700–2711.
- Zelensky, A.N., Sanchez, H., Ristic, D., Vidic, I., van Rossum-Fikkert, S.E., Essers, J., Wyman, C., Kanaar, R., 2013. Caffeine suppresses homologous recombination through interference with RAD51-mediated joint molecule formation. *Nucleic Acids Res.* 41, 6475–6489.
- Zhang, Q., Zhang, F., Li, S., Liu, R., Jin, T., Dou, Y., Zhou, Z., Zhang, J., 2019. A multifunctional nanotherapy for targeted treatment of colon cancer by simultaneously regulating tumor microenvironment. *Theranostics* 9, 3732–3753.
- Zhou, P., Wu, X., Chen, H., Hu, Y., Zhang, H., Wu, L., Yang, Y., Mao, B., Wang, H., 2020. The mutational pattern of homologous recombination-related (HRR) genes in Chinese colon cancer and its relevance to immunotherapy responses. *Aging (Albany NY)* 13, 2365–2378.